Hindawi
International Journal of Aerospace Engineering
Volume 2023, Article ID 1773841, 20 pages
https://doi.org/10.1155/2023/1773841

Research Article

Landing Reliability Assessment of Airdrop System Based on Vine-Bayesian Network

Wei Cheng,[1] **Chunxin Yang**,[1] **and Peng Ke**[2]

[1]*School of Aeronautical Science and Engineering, Beihang University, Beijing 100191, China*
[2]*School of Transportation Science and Engineering, Beihang University, Beijing 100191, China*

Correspondence should be addressed to Peng Ke; p.ke@buaa.edu.cn

Received 14 July 2022; Revised 21 March 2023; Accepted 13 April 2023; Published 29 April 2023

Academic Editor: Paolo Castaldi

The landing phase of an airdrop process is prone to accidents, and thus, it is important to assess the landing reliability for an airdrop system. However, full field tests to assess the reliability are unacceptable due to their cost and the time required. As such, it is necessary to estimate the reliability in the design stage. To address this problem, a method based on vine-Bayesian Network (vine-BN) is proposed to assess the landing reliability by fusing multisource information. First, the network structure is determined by the relationship between data of simulation or ground tests and failure modes. Then, nodes are defined as random variables on [0, 1] based on the definition of the performance metric. Finally, the dependence between nodes is quantified by expert opinions. To illustrate the effectiveness of the method, a particular ground test or simulation is chosen to establish a network for a typical heavy cargo airdrop system (HCADS). Forward and backward propagation is carried out on the network. The forward analysis predicts the landing reliability in the design stage through multisource information fusion. Beta distribution is applied to fit the fusion result, so Bayesian inference is made to perform field test times decision-making. The backward analysis works to identify the key performance metrics related to landing reliability. The results and analysis manifest that vine-BN is feasible for fusing multisource information. Through the network, the reliability of the current design can be predicted effectively, and the field test times can be remarkably reduced. This method plays a crucial role in airdrop system design and reducing test time and labor.

1. Introduction

The airdrop system is a typical complex parachute system. It is aimed at ensuring that the payload lands safely with speed and attitude requirements and plays a crucial role in military applications, large-scale humanitarian aid, spacecraft tests, and planetary exploration. Due to the unsteady aerodynamic environment and the flexible parts, the whole airdrop process is characterized by nonlinear and high uncertainty, which is unfavorable for the airdrop mission. The airdrop process can be divided into four major phases: extraction, parachute deployment, steady descent, and landing. In the extraction process, due to the unsteady flow around the aircraft, the initial motion of the payload varies, thus affecting the subsequent process. This phenomenon is prominent in personnel airdrop [1], which will lead to personal injury and nonrepeatable airdrop missions [2, 3]. During parachute deployment, high-altitude wind usually causes line sail or whipping phenomenon, which may lead to damage of the parachutes [4]. In the steady-descent process, parachute collision usually occurs in parachute clusters, resulting in structural deformation of the canopy, thus influencing the aerodynamic characteristic and the system motion states. This problem involves fluid-structure interaction, which is quite complicated [5]. The landing phase is the final phase of the airdrop process and is prone to accidents such as rollovers and overloading. Besides the uncertainty of the previous phases, various factors affect landing, among which the most significant are the landing terrain and wind field, as well as the motion states at the moment of landing. For the precision airdrop systems, the landing accuracy should be considered [6].

Quantitative assessment of the risk of airdrop missions due to uncertainties is of interest for system performance

and design. Due to cost and time, it is unacceptable to perform statistical probability estimation that only relies on field tests. In addition, it is necessary to conduct a reliability assessment in the design stage, where there is no field test data. The existing research on the quantitative evaluation of the success of a drop mission focuses on Monte Carlo Simulations (MCS). Wachlin and Costello [7] performed MCS based on a 6-DOF dynamic model for a guided airdrop system equipped with a trailing edge control parafoil and bleed air control parafoil, and they regarded the wind speeds and directions along with the ground contact parameters as uncertainty factors to investigate the probability characteristic of impact acceleration and rollover in the landing process. In planetary exploration, landing stability or landing site selection are commonly conducted based on MCS. Dong et al. [8] established a dynamic model for a Mars lander with attitude control thrusters. Their probability analysis emphasized the influence of irregular terrain. Due to the unavailable data of Mars, lunar terrain data was used to simulate terrain characteristics for Mars in order to conduct MCS for landing stability. Witte et al. [9] established a dynamic touchdown model for the Philae lander, and they performed MCS with velocity, attitude angle, and flight path angle input as uncertainty parameters. Compared with the MCS results, which considered landing stability and energy absorption criteria, the optimal landing site was determined. In terms of test studies, drop tests are generally performed to investigate the landing uncertainty at the moment of landing for different initial motion states. Lee et al. [10] designed a subscale drop test for the Orion Crew Exploration Vehicle (CEV). The test device allows for easy adjustment of landing conditions, and Lee conducted more than 60 drop tests to simulate potential landing conditions. While MCS can provide a probabilistic analysis of the uncertainty of the airdrop process, some drawbacks limit its further application. First, the accuracy of the probabilistic analysis is limited by the simulation model or the test method. Second, MCS can only reflect the effects of a limited number of specific uncertainty factors, whereas the actual airdrop process involves a large number of uncertainty factors connected in complex ways that would make MCS too complex to implement. In addition, statistical laws for the uncertainty factors are difficult to obtain or even to describe statistically. Third, it is computationally demanding for MCS applications, which is prominent in the assessment of the landing process. Many airdrop systems use airbags for landing buffers, and finite element methods are often used to model the airbag buffer process [11–13], which can simulate instantaneous deformation with high precision but with less computational efficiency. If the MCS were to be used to analyze the buffering characteristics under different landing conditions, it would face a massive computational effort.

Therefore, it is not sufficient to analyze the landing probability properties based on MCS alone. Several researchers have proposed to use the Bayesian method with simulations or ground tests as prior information, further combined with limited field tests, to evaluate the reliability of an airdrop system. On the one hand, it can reduce the field test times, and on the other hand, it can enable the fusion of different pieces of information to give more reasonable evaluation results. NASA [14] used a Bayesian approach to evaluate the failure probability of the Orion CEV Parachute Assembly System (CPAS), in which the prior information came from the historical airdrop test data of the Soyuz parachute system, the Apollo parachute system, and the military airdrop system. Gao et al. [15] constructed a fluid-structure interaction (FSI) model for the inflation of a slot parachute used in military airdrop missions to address the problem of reliability assessment of inflation. The Bayesian approach was used to reduce the experimental data on inflation by taking the structure strength data obtained from the FSI simulation as prior information. Ma et al. [16] selected test data from different units as prior information for an emergency escape parachute system. The prior distribution was built from the zero-failure and with-failure cases for all prior data. The posterior distribution of the emergency escape parachute system was then determined by the Bayesian approach to further assess reliability. In this work, only the case where the prior pieces of information were binomial data was considered. It can be seen that the limitations of the aforementioned studies based on the Bayesian method to evaluate the reliability of airdrop systems are in the choice of prior information. The prior information either is limited to binomial data or relies only on a single information source.

The prior pieces of information of the airdrop system are complementary to each other and exist in different data types. Extensive ground tests and simulations are carried out during the design stage to investigate the uncertainty characteristics of airdrop systems. After the design is completed, field tests will be conducted to comprehensively evaluate the performance of the airdrop system despite its small sample size characteristics. In addition, prior information also includes expert opinion, which is derived from extensive engineering experience. NASA has emphasized expert opinion in the design of CPAS [17]. Generally, expert opinion is widely used in the area of reliability assessment, differing only in the form of elicitation. Therefore, there is a large amount of available prior information for the airdrop system. However, some existing studies that use the Bayesian method to evaluate the reliability of airdrop systems have implemented information fusion, but the limitation lies in the fusion of either a single information source or binomial data type. The essence of the MCS commonly used in uncertainty analysis of airdrop systems is to evaluate the airdrop uncertainty using a single piece of information, without information fusion. As a result, existing studies on uncertainty assessment of airdrop systems do not fully exploit multisource information. The integration of multisource information will provide a deeper insight into the uncertainty of the airdrop process, which involves information fusion issues.

The Bayesian network (BN), as a tool for uncertainty, has been fully explored for its probabilistic inference capability. BN is also able to effectively integrate information from multiple sources and has been widely used in the field of reliability assessment, fault diagnosis, etc. Sun et al. [18] used a BN model to fuse health parameters and monitoring signals to improve the performance of gas path analysis. Chen and

Liu [19] integrated multimodal surface measurements through a BN to estimate the strength of aging material. Junghans and Jentschel [20] applied a BN to integrate sensor measurement data and conditional data of the sensor in traffic surveillance to improve the accuracy of vehicle classification. Through the fusion of information using BNs, Cai et al. [21] performed a fault diagnosis of the ground source heat pump with increased accuracy. Nevertheless, the variables of the BNs in these studies were discrete, and the network was parameterized using conditional probability tables (CPTs). With the increase of nodes, the CPTs become large and complicated. This drawback will be prominent when continuous nodes are discretized, which limits further application of BNs. The nodes in a Gaussian Bayesian network can be continuous, but the restriction to joint normality is highly severe. Though mathematical tricks can be applied to transform the nodes to normal, the partial regression coefficient on each arc corresponds to the normal node, rather than the original one, which leads to difficulty in correlation elicitation.

To overcome these hurdles, Kurowicka and Cooke [22] proposed a method called a vine-BN based on the theory of vines [23, 24]. The vine-BN is nonparametric, and the nodes are associated with arbitrary continuous invertible distribution and connected by copula functions. The rank correlation on each arc is realized by a copula function, and it is invariant under monotone transformations. Due to these advantages, applications of vine-BN's probabilistic inference capability have increased in the field of reliability analysis and risk assessment in the last decade. Morales-Napoles et al. [25] investigated earth dam safety and analyzed the causes and consequences of earth dam failure. Zilko et al. [26] constructed a railway-disruption-length prediction model. Lee and Pan [27] presented an approach to a reliability assessment of an automated production line of lithium batteries at the early design stage. Mendoza-Lugo et al. [28] established the failure probability mode of concrete vehicle bridge columns under the combination of traffic load and seismic activity. Pan et al. [29] developed a structural health model of underwater tunnels. Sun et al. [30] constructed a network model to assess the risk of water inrush for a tunnel. As for the research on the information fusion of vine-BN, to our knowledge, there has been no literature published yet.

In this paper, a method to assess the landing reliability of a typical HCADS based on information fusion via the vine-BN method is proposed, where the information comes from the ground test of components, the simulation, and the expert opinions. Multiple ground tests are usually conducted on the same component to investigate the impact on the landing process from different angles. Meanwhile, the same ground test or simulation model may provide multiple data to predict different failure modes. Performance metrics of ground tests and simulations can be regarded as symptoms, and different landing accidents are faults. The correlations between them are elicited by expert opinions. Therefore, our proposed method is based on multisource information fusion, which can provide more reasonable results. The fusion is implemented by the forward propagation of the network. Fusion results can be taken as prior knowledge of landing reliability. Once the field test data (usually a limited sample) are available, Bayes inferences can be made based on the fusion results to obtain a posterior distribution of landing reliability. Backward propagation on the network recognizes the performance metrics that make a significant contribution to landing reliability, thus providing guidelines for system design. Table 1 shows a brief comparison of existing research methods and our proposed approach.

The rest of the paper is organized as follows: Section 2 describes the system configuration and airdrop process of a typical HCADS in detail and briefly introduces the ground test and simulation information needed to build the network; since our study mainly focuses on the fusion of simulations and ground tests, the detailed test method and simulation model will not be covered. Section 3 illustrates the basic theory of vine-BN, mainly including pair copula decomposition, vines, and the sampling algorithm. Section 4 constructs the network for landing reliability, including network structure, node definition, and network quantification. Section 5 demonstrates the application in landing reliability analysis using the network from forward propagation and backward propagation. Finally, the conclusion and future work are presented in Section 6.

2. Landing Reliability of the HCADS

2.1. Airdrop Process and System Configuration of HCADS. Figure 1 illustrates the whole airdrop process of a typical HCADS. The whole process can be divided into four phases briefly. First, the cargo platform extracts out of the cargo bay by the aerodynamic force of the extraction parachute. Then, the main parachute system, which is composed of four main parachutes and four drogue parachutes, is deployed by the pilot parachute. After deployment, the system decelerates quickly to the steady-descent phase. Finally, the cargo lands with a cushioning airbag.

2.2. The Formation and Causes of Landing Failure. Landing failure may occur in three modes, including exceeding the cargo overload limit, cargo rollover, and airbag structure failure. The parachute-release process and airbag-buffering process occur simultaneously and interact with each other. In the following section, we will thoroughly analyze the factors that lead to the failure of the landing during the two processes.

2.2.1. Release Process. To protect the landing failure of the cargo rollover, the cargo-hanging rope and the parachute-connecting rope are connected by the release unit, which ensures the disconnection of the parachute and cargo platform automatically at the moment of landing. Figure 2 shows the physical image and the structure sketch of the release unit.

The automatic release process can be divided into three stages: First, before cargo extraction, the spring is compressed to an initial tightening position, and the latch is fixed by pyrotechnics. Then, when the cargo is extracted and reaches a steady-descent state, the pyrotechnics explode;

Table 1: Comparison of the proposed method with existing studies on the uncertainty of the airdrop process.

	Existing research		The method proposed in this study
	MCS method	Bayesian method	Vine-BN method
Advantages	Easy to implement	Information fusion; reduction of the number of field tests	(1) Multisource information fusion (2) No data type restriction (3) Key performance metric identification
Disadvantages	(1) Depends on the accuracy of the simulation or test method (2) Statistical laws for the uncertainty factors are difficult to obtain or even to describe statistically (3) Computationally demanding for application	(1) Single-source information (2) Constraint of data type	

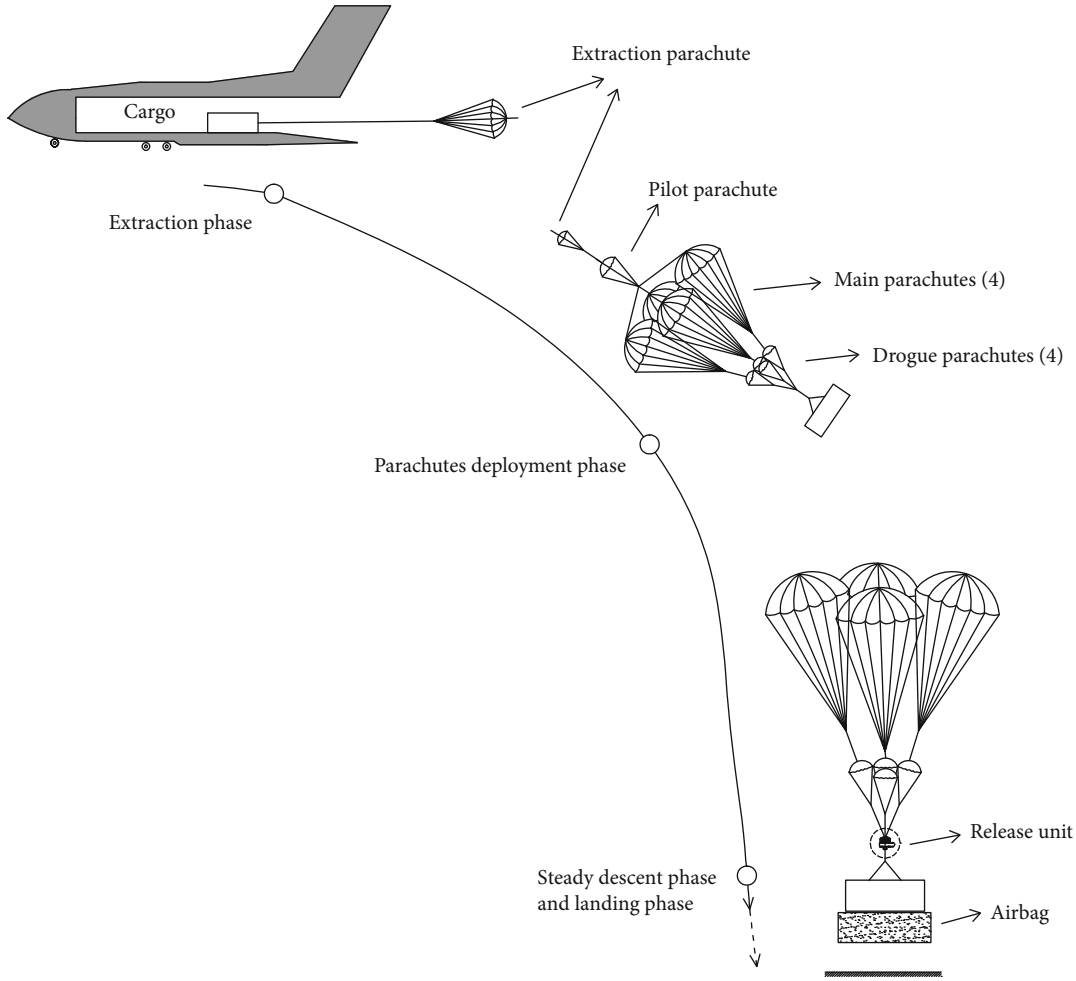

Figure 1: Airdrop process of a typical HCADS.

thus, the tension of the parachute-connecting rope and the cargo-hanging rope causes the hanger and pull ring to press against the latch, and a large static friction force is generated to keep the release unit locked. Finally, the static friction force on the latch reduces when the rope tension unloads quickly at the moment of landing; the latch is, hence, ejected under the spring force, and the cargo and the parachute are separated.

Figure 3 schematically describes the key time points in the release process on the time axis.

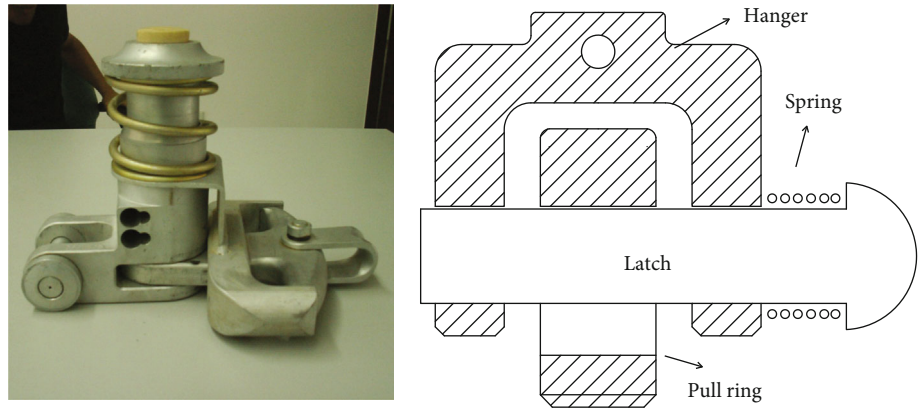

(a) Physical image (b) Sketch of the structure

Figure 2: Release unit.

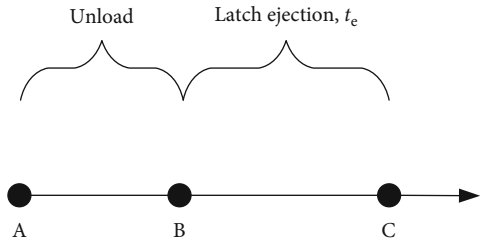

Figure 3: Release process.

(1) Stage AB: stage AB is the rope tension force–unloading process. The rope tension force at point B is denoted as the design release force T_s and is a key design parameter. The process is complicated and determined by the initial motion state at the moment of landing and interacts with the buffering process. In addition, the aerodynamic force has a remarkable influence on the rope tension force, so the parachute collision and wind field should be considered

(2) Stage BC: to ensure safety separation, the latch-ejection response time t_e should be as small as possible. Due to the machining precision, the surface roughness of the release unit and the spring stiffness are variable, which directly affect t_e

2.2.2. Buffering Process. Cargo rollover or exceeding the overload limit may occur in the buffering process due to landing terrain and initial motion state at the moment of landing. The airbag-rebound problem can also lead to uncontrollable attitude and secondary shock in the landing process, leading to cargo rollover and exceeding the overload limit. In the worst case, airbag peak pressure above a specified threshold can lead to airbag structure failure.

2.3. Data Collection for Assessing Landing Reliability. According to the above analysis, Figure 4(a) shows comprehensive factors and the corresponding landing-failure modes. Note that the above qualitative analysis is derived from extensive engineering experience. More comprehensive factors can be determined via simulation or testing. The purpose of this article is to fuse different pieces of information from those simulations and tests to evaluate landing.

Due to the limitations of test conditions and the simulation model, we will introduce typical ground tests and a simulation model from the simplified factors shown in Figure 4(b). Specified data will be extracted from the simulation and ground test to evaluate the landing. Note that this paper is aimed at proposing a general framework to assess the landing reliability for an airdrop system. The specific test methods and simulation models are beyond the scope of this paper. The following only introduces several typical tests and a simulation model to pave the way for the construction of the methodology in subsequent sections.

2.3.1. Data Collection for Release Process

(1) Release Simulation. The purpose of the release simulation is to investigate the failure of cargo rollover under the factors of wind field, initial motion state, and rope tension force. Wang et al. [31] proposed a release simulation model for stage AB in Figure 3, and they only considered the influence of the parachutes' initial motion state and wind field of the landing site. The release process is considered a success when the rope tension force is smaller than the design release force T_s, in which case the cargo rollover at landing would not occur. This model will be used in our research. Full details are given in the appendix.

(2) Release Unit Test. The purpose of the release unit test is to investigate the failure of cargo rollover under the factor of latch-ejection response time. As discussed above, the latch-ejection response time varies with machine errors and is critical to landing. It is imperative to arrange a ground test of the release unit to determine the statistical law of the latch-ejection response time caused by machining errors,

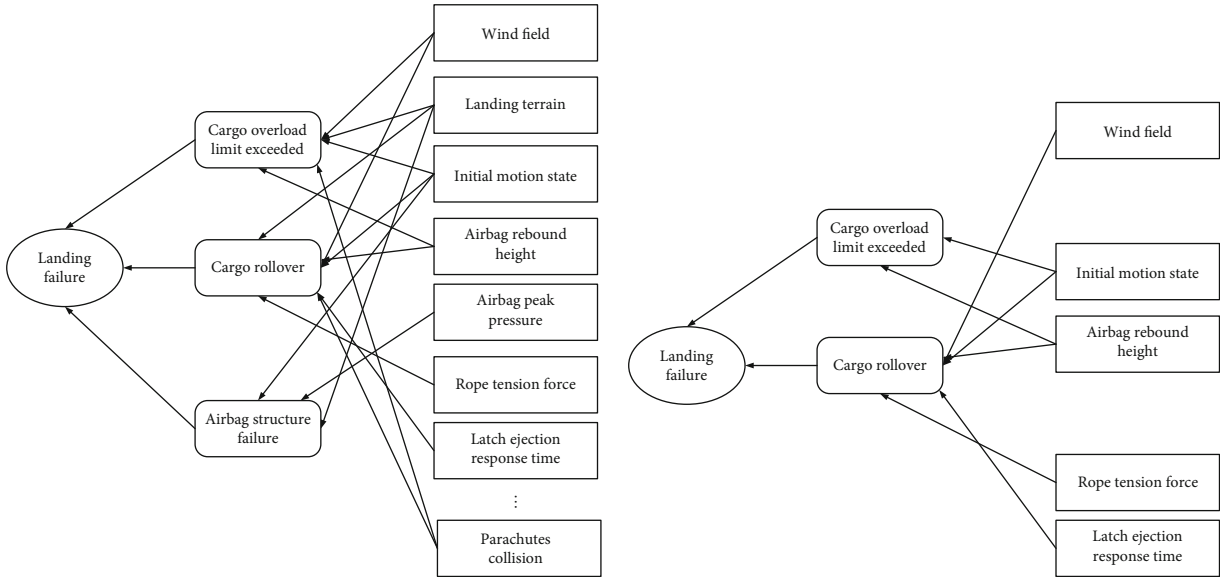

(a) Comprehensive factors (b) Simplified factors

Figure 4: Factors causing landing failure.

and the performance target t_0 should be specified by the designer. The case in which the latch-ejection response time is greater than t_0 indicates the risk of cargo rollover at landing. Note that the machining accuracy uncertainty is pervasive, and only the factors that play a substantial impact on successful landing should be concerned.

2.3.2. Data Collection for Buffering Process. The purpose of the airbag drop test is to investigate the failure of cargo rollover and overload limit exceeded under the factors of initial motion state and airbag-rebound height. In some studies on spacecraft-landing uncertainty, drop tests are usually used to investigate the influence of the terrain and the motion states on landing [10, 32, 33]. Similarly, the drop test can be conducted for HCADS. A large number of drop tests are needed to investigate the landing reliability under different initial motion states at the moment of landing. Lee et al. [10] designed a subscale drop test for the Orion Crew Exploration Vehicle. The test device can easily adjust the landing conditions, and Lee et al. conducted over 60 drop tests to simulate the potential landing conditions. The test method can also be applied to the ground test for HCADS, and the test configuration is shown briefly in Figure 5 Three pieces of data should be of concern: the rebound height, the overload, and the rollover cases of the airdrop test. The performance targets of the rebound height and overload are also specified by the designer. That is, if the overload or the rebound height is greater than the performance target G_0 or h_0, respectively, the risk of landing failure increases.

To sum up, we will evaluate the landing reliability with the information of the ground test and simulation shown in Table 2 in subsequent sections.

The relationship between collected data and failure modes can be specified by probabilistic dependence, which can be constructed through vine-BN.

3. Basic Theory of the Vine-BN Method

Vine-BN is a combination of BN and a vine. A vine provides a decomposition form of a multivariate joint distribution, and the specific structure of the BN simplifies the decomposition of the vine and its sampling algorithm. In the following section, we first introduce the basic theory of vines and then illustrate how the vine is combined with the BN.

3.1. Vine

3.1.1. Decomposition Form. A joint distribution function implies not only the marginal distribution of each variable but also the degree and the structure of the correlation between them. According to Sklar's theorem [34], any joint density function can be decomposed into an n-dimensional copula function and n univariate marginal distribution functions.

$$F(x_1, x_2, \cdots, x_n) = C(F_1(x_1), F_2(x_2), \cdots, F_n(x_n)). \quad (1)$$

The density function form of Equation (1) is

$$f(x_1, x_2, \cdots, x_n) = c(F_1(x_1), F_2(x_2), \cdots, F_n(x_n)) \prod_{i=1}^{n} f_i(x_i), \quad (2)$$

where c represents the derivative of the corresponding copula function.

Since the n-dimensional copula function can also be regarded as the cumulative distribution function on $[0, 1]^n$, its derivative is also the probability density function. The dependency and structure between variables are characterized by the copula function. Therefore, through the copula function, we can study the marginal distribution and the dependency separately and reduce the difficulty of modeling

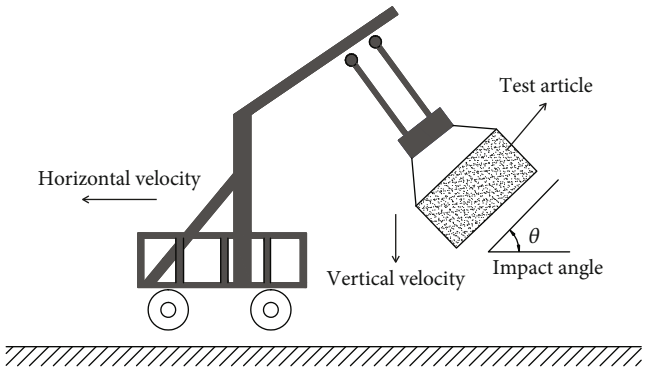

Figure 5: Subscale drop test [10].

and analyzing a multivariable probability model. As the dimension grows, the copula function has a limited ability to describe the dependency among variables, and the solution of its derivative function is also very complex. To tackle this issue, Bedford and Cooke [24] proposed a pair-copula decomposition method based on Joe's work [35], which essentially decomposes the joint density function into the product form of multiple bivariate copula functions and each marginal density. This method is more flexible in multidimensional distribution modeling. Since such decomposition can come in various forms, Bedford and Cooke [23] further proposed a graphical modeling tool, the vine, to describe the logical structure of a particular type of decomposition. A vine consists of many trees, and each tree has many nodes. The line connecting nodes is called an edge. The nodes and edges form a set jointly, which can be combined in different ways to constitute a vine. A vine also comes in many forms, and one is called a D-vine, which is directly related to vine-BN. Here, we take the four-dimensional decomposition as an example to show the D-vine.

In the D-vine, nodes represent variables, edges represent copula functions that connect two nodes, and the edge of the i-th tree becomes the node in the $i+1$-th tree. As shown in Figure 6, nodes 1 and 2 on tree T1 represent variables 1 and 2, respectively. They are connected by edge 12, and their copula density function is denoted as c12. Nodes 12 and 23 in tree T2 are also edges 12 and 23 in tree T1, and they are connected by edge 13|2, which indicates that nodes 1 and 3 are connected with node 2 as the conditional variable, and their copula density function is denoted as c13|2. According to this rule, the D-vine decomposition of the four-dimensional density function can be written as

$$\begin{aligned} &f(x_1, x_2, x_3, x_4) = f_1(x_1) f_2(x_2) f_3(x_3) f_4(x_4), \\ &c_{12}\{F(x_1), F(x_2)\} c_{23}\{F(x_2), F(x_3)\} c_{34}\{F(x_3), F(x_4)\}, \\ &c_{13|2}\{F(x_1|x_2), F(x_3|x_2)\} c_{24|3}\{F(x_2|x_3), F(x_4|x_3)\}, \\ &c_{14|23}\{F(x_1|x_2, x_3), F(x_4|x_2, x_3)\}. \end{aligned} \tag{3}$$

The essence of the D-vine decomposition is to describe the overall dependency structure through the (conditional) dependency between any two variables.

3.1.2. Sampling Algorithms. The general principle for sampling a vine is as follows.

Set the sampling order as $x_1, x_2, \cdots, x_n$. For convenience, we assume that the variables are uniform at $[0, 1]$. The sampling formula is then

$$\begin{cases} x_n = u_1, & n = 1, \\ x_n = F^{-1}(u_n | x_1, x_2, \cdots, x_{n-1}), & n > 1, \end{cases} \tag{4}$$

where u_n is the uniform random number on $[0, 1]$. For a D-vine, the conditional function is determined by the following equation [36]:

$$F(x_j | x_1, \cdots, x_{j-1}) = \frac{\partial C_{j,1|2,\cdots,j-1}\{F(x_j | x_2, \cdots, x_{j-1}), F(x_1 | x_2, \cdots, x_{j-1})\}}{\partial F(x_1 | x_2, \cdots, x_{j-1})}. \tag{5}$$

The implementation of the algorithm is a recursive process of Equation (5). Kurowicka and Cooke [37, 38] used a graphical structure to describe this process, which will not be covered here. In the following section, we will see that vine-BN is a combination of BN topology and D-Vine decomposition: BN topology introduces conditional independence for D-vine decomposition, thus simplifying its decomposition structure and the corresponding sampling algorithm.

3.2. Vine-BN

3.2.1. Brief Introduction to BN. According to the chain rule, a joint probability density can be factorized as

$$f(x_1, x_2, \cdots, x_n) = f(x_1) \prod_{i=2}^{n} f(x_i | x_1 \cdots x_{i-1}). \tag{6}$$

The BN is a directed acyclic graph. Nodes represent univariate random variables, and arcs represent the direction of influences. Based on the (conditional) independence statements encoded in the BN, Equation (6) can be simplified as

$$f(x_1, x_2, \cdots, x_n) = \prod_{i=1}^{n} f\left(x_i \middle| x_{\mathrm{Pa}(i)}\right), \tag{7}$$

where $x_{\mathrm{Pa}(i)}$ represents the parent node of x_i. Equation (7) shows that the BN is another concise, yet complete, representation of the joint probability distribution [39]. The decomposition also has a corresponding discrete form. In the discrete BN, marginal distributions specify the root nodes, and the child nodes are specified by the CPTs. CPTs are also used to characterize the dependency between nodes. In vine-BN, rank correlations are assigned to arcs to measure the strength of the connection between nodes, whose definition is below.

Table 2: Simulation and ground tests for assessing landing reliability.

Simulation or ground test	Collected data	Performance target	Failure mode
Release simulation	Release or not in simulation (RNS)	Yes	Cargo rollover
Release unit test	Latch-ejection response time via ground test (LERTGT)	$LERTGT < t_0$	Cargo rollover
Airbag drop test	Drop test overload (DTO)	$DTO < G_0$	Overload limit exceeded
	Drop test rebound height (DTRH)	$DTRH < h_0$	Overload limit exceeded, cargo rollover
	Rollover or not in drop test (RNDT)	No	Cargo rollover

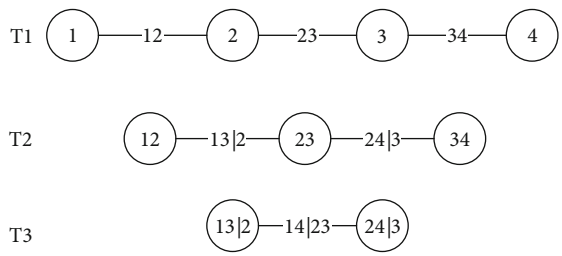

Figure 6: D-vine decomposition on four variables.

3.2.2. Measure of Dependency. The rank correlation, or Spearman correlation, of two random variables is defined as follows [24]:

$$r(X, Y) = \rho(F_X(X), F_Y(Y)), \tag{8}$$

where F_X and F_Y are the cumulative distribution functions of X and Y, respectively. ρ is the Pearson correlation, also called the product moment correlation, which is defined as follows.

The Pearson correlation of random variables X and Y, with expectations $E(X)$ and $E(Y)$ and variances σ_X^2 and σ_Y^2, is expressed in the following equation:

$$\rho(X, Y) = \frac{E(XY) - E(X)E(Y)}{\sigma_X \sigma_Y}. \tag{9}$$

That is, the Spearman correlation of the variables X and Y are equal to the Pearson correlation of their distribution functions. The rank correlation is a measurement of the dependence between two random variables, and it can be realized using any copula that has the zero-independence property; i.e., any copula that represents (conditional) independence as a zero (conditional) rank correlation. Furthermore, the rank correlation measures the strength of the monotonic relationship between two random variables. It is invariant under a monotone transformation, and the nonlinear relationship can be measured by it.

The concept of conditional rank correlation is vital in vine-BN, which refers to the correlation of X and Y given Z, defined as [40]

$$r(X, Y|Z) = r\left(\tilde{X}, \tilde{Y}\right), \tag{10}$$

where $(\tilde{X}, \tilde{Y})$ represents the conditional distribution of (X, Y) given Z.

3.2.3. Combination of Vine and BN. Vine-BN is parameterized by a (conditional) rank correlation. Assume that node i has $p(i)$ parent nodes. The correlation on each arc is then given by the following equation:

$$\begin{cases} r\left(i, i_{p(i)}\right), & k = 0, \\ r\left(i, i_{p(i)-k} \middle| i_{p(i),\cdots,i_{p(i)-k+1}}\right), & 1 < k < p(i) - 1. \end{cases} \tag{11}$$

Kurowicka and Cooke [22] proved that, using a BN with continuous invertible distribution nodes specifying (conditional) rank correlations (11) through the zero-independence copula, the structure of the BN uniquely determines a joint distribution, and the correlations are algebraically independent.

Due to the (conditional) independence implied by the BN, the correlation between any child node and its non–parent node is zero, so the corresponding copula density function $c(\bullet,\bullet) = 1$. Thus, the D-vine decomposition can be simplified.

Vine-BN sampling is accomplished by building a corresponding D-vine. First, set the sampling order: start with root nodes and end with leaf nodes. Afterward, let D_i denote the D-vine on node i, i.e., sampling node i by the method for sampling D_i. Because of the conditional independence, only the parent nodes of i are needed to construct D_i.

The sampling order for Figure 7(a) can be 12345 or 13245. D_4 is constructed for sampling node 4, as shown in Figure 7(b). The node order in the first tree of the D-vine corresponds to the correlation specification in the BN; for example, an alternative correlation specification can be $\{r21, r31, r42, r43|2, r54\}$, and nodes in the first tree of D_4 can then be placed as $\{4, 2, 3\}$.

4. Network Modeling of Landing Reliability

4.1. Network Structure of Landing Reliability. When a product is in the design stage or there is no field data available, the system-level performance is usually evaluated by simulation or component tests before the decision analysis. In other words, simulation or component-level tests are used to predict possible failures. Therefore, data provided by simulation and ground tests can be regarded as symptoms, and different landing accidents are faults. The relationship

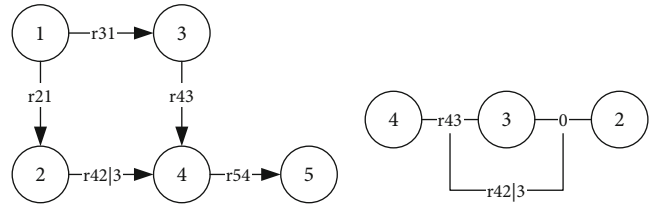

(a) BN with five nodes (b) D_4 for sampling variable 4

Figure 7: Illustration of the BN and the corresponding sampling D-vine.

between the symptoms and faults can be described by probabilistic dependence. Based on this idea, a general network for inferring the landing performance is shown in Figure 8(a). More specifically, according to the analysis in Section 2 and the available information in Table 2, the network structure for the landing reliability of HCADS is simplified as Figure 8(b).

4.2. Node Definition of Landing Reliability Network: Performance Metrics for Collected Data. Since the copula function is defined in $[0, 1]$, the nodes in vine-BN need to be converted to the distribution on $[0, 1]$. Some studies [25, 26, 29] transformed each node to $[0, 1]$ through cumulative distribution functions (CDFs), and the original distribution was then converted back from their inverse CDFs. In this research, we define the nodes as random variables on $[0, 1]$ directly. In terms of each piece of data shown in Table 2, the probability of meeting the performance target determines the system performance. Therefore, the root nodes are defined as the probability of meeting the performance target, which can be regarded as a continuous random variable on $[0, 1]$. In the following, we refer to the probability as the performance metric for data collected from simulations or ground tests. It can obtain a random variable on 01 for any type of data through the definition of the performance metric on which information fusion is based. Therefore, the method is not constrained by the data type of the information source, and data collected from simulations or ground tests can be of any type. Take root node LERTGT for instance; the performance metric can be defined as the following equation:

$$\text{Node}_{\text{LERTGT}} = P(\text{LERTGT} \le t_0). \tag{12}$$

$\text{Node}_{\text{LERTGT}}$ can be regarded as a continuous random variable on $[0, 1]$. When the data of the simulation and ground test is not available, it is legitimate to model the performance metrics as uniformly distributed. Once the data are available, the distribution or the estimation of the performance metrics can be determined. However, it is usually difficult to determine the distribution of performance metrics. On the other hand, since vine-BN can be updated with values or intervals, there is no need to specify the distribution of performance metrics, but only an estimation with available data is needed. For success/failure data, such as RNDT, the estimation is straightforward. For continuous data, such as LERTGT, the estimation can be determined through the probability density function (PDF) with available data. The PDF can be determined by the parametric method and the nonparametric method. The former assumes that the form of PDF is given, and the parameters are estimated. This method relies on prior assumptions about the population. The nonparametric method does not specify the distribution of population, and the PDF is directly determined by data. The kernel density estimation (KDE) is a nonparametric method. When the observations of variable X are available: $\{x_1, x_2, \cdots, x_n\}$, the PDF of X can be given by the following equation [41]:

$$\widehat{f}_h(x) = \frac{1}{nh}\sum_{i=1}^{n} K\left(\frac{x - x_i}{h}\right), \tag{13}$$

where h is the bandwidth and K is the kernel function.

Note that the sample size of the simulation results can be infinite, so the probability can be estimated directly from the data. For the ground test, although the sample is not small, it is also relatively limited. In this case, the nonparametric bootstrap method can be used to improve estimation accuracy. For details, we refer the readers to literature [41].

4.3. Quantification of Dependency between Nodes. In this section, we elicit the correlations on the arcs of Figure 8(b). Before elicitation, the type of copula function must be specified. Copula functions differ in many properties, such as symmetry and tail behavior [34], which will lead to different reliability assessment results. There are several commonly used copula functions, such as Gaussian, Clayton, Frank, and Gumbel. Clayton was assigned to each arc of the network. The expression of the bivariate Clayton density function is as follows:

$$c(u_1, u_2) = (1 + \delta)(u_1 u_2)^{-1-\delta}\left(u_1^{-\delta} + u_2^{-\delta} - 1\right)^{-1/\delta - 2}. \tag{14}$$

The assignation was based on the following phenomena: Simulation and component-level tests are generally performed first, and if the results prove to be reliable, field tests are carried out to evaluate the system performance further. However, if the simulation and component-level test results are not satisfactory, the system will be adjusted until the simulation or component-level test results show satisfactory performance before the field test. In other words, when the reliability of the simulation and ground test results is low, the possibility that the system has low reliability is considerable. If the simulation and ground tests perform well, the system does not necessarily have high

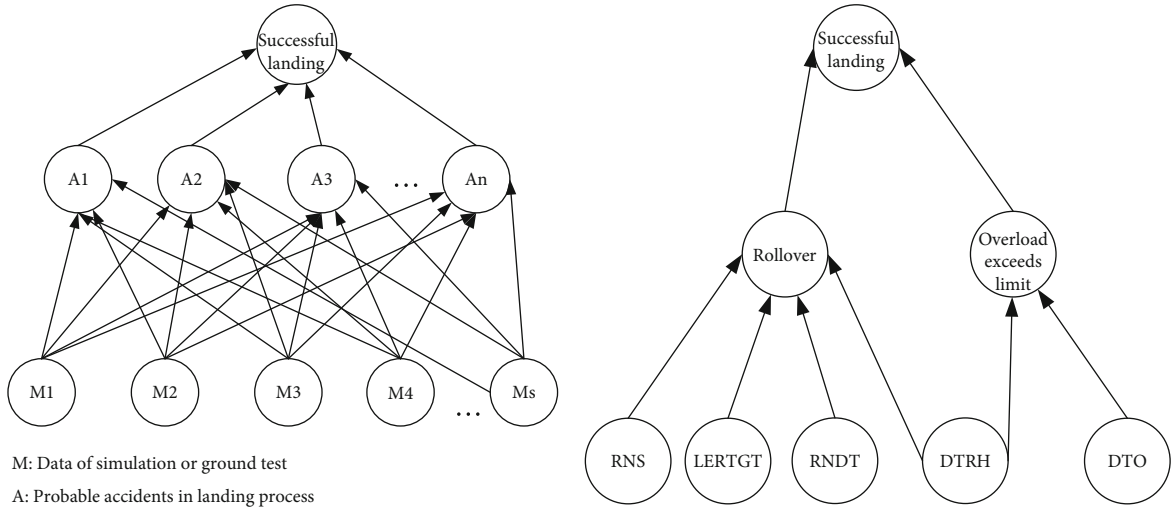

(a) General network structure

(b) Simplified network for a typical HCADS

Figure 8: Network structure for evaluating landing reliability.

reliability. This characteristic corresponds to the lower-tail dependence behavior of the Clayton function, which is demonstrated in Figure 9.

Figure 9 shows the sample generated by a bivariate Clayton copula function with a rank correlation of 0.8. It shows that, when the values of these two variables are small, they have a stronger correlation, which is due to a lower-tail dependence.

Moreover, the Clayton copula function can only specify a positive correlation, which is consistent with the network shown in Figure 8(b); that is, any child node has a positive impact on its parent node. The higher the performance of any simulation or test results, the more reasonable it is to consider that the landing is safe.

Expert judgments are regularly used in helping reliability modeling when data is insufficient. With regard to discrete BN, expert judgments are for instantiation [42], i.e., specifying the conditional probabilities. For the vine-BN correlation, the instantiation is accomplished by eliciting the correlation. The elicitation can be achieved by assessing the exceedance probability [40]. It is unintuitive for specialists when the number of parent nodes is large. An alternative way to elicit the correlation is to assess the exceedance probability for unconditional rank correlation; then, the conditional rank correlation can be elicited through the ratio of unconditional rank correlation [25].

For illustration, we numbered the nodes in Figure 8(b) and assigned a (conditional) correlation to each arc according to Equation (11), as shown in Figure 10. When updating the network, the number also corresponds to the sampling order.

The assessment started from the unconditional rank correlations, such as $r61$. The experts were asked the following question, which we denote as question 1: "If the simulation results show that the release probability (Node 1) is greater than 0.5, then what is the probability that the reliability of no rollover during the actual landing (Node 6) is also greater than 0.5?" That is, this question requires experts' estimation of P_1:

$$P_1 = P(X_6 > 0.5 | X_1 > 0.5). \tag{15}$$

Question 1 was answered by three experts, and the mean value was taken as P_1, which satisfied the following equation:

$$P_1 = \frac{1}{1-0.5}\int_{0.5}^{1}\int_{0.5}^{1} f_{61}(X_1, X_6)\,dX_6\,dX_1. \tag{16}$$

The parameter of the Clayton copula function can be obtained through Equation (16), so the correlation $r61$ can be determined. According to the assessment, $P_1 = 0.670$, and $r61 = 0.4868$.

Then, the corresponding question to elicit $r62|1$ is denoted as question 2: "Given previous results, what is the ratio of $r62/r61$?" The ratio will be restricted by $r61$. Due to the algebraic independence of correlations entailed in Equation (11), $r62|1$ can take any value in $[0, 1]$. So the range of $r62/r61$ can be determined through simulation by building the D-vine on X_1, X_2, and X_6. In this way, Figure 11 shows the relationship of $r62/r61$ to $r62|1$.

As the figure depicts, the experts will be required to determine the ratio of $r62/r61$ in the approximate range of $[0, 1.7]$. The red mark in the figure marks the mean value evaluated by three experts, and thus, $r62|1$ can be determined. In this way, the network was quantified, as shown in Figure 12.

Note that a high-precision simulation model can provide a more insightful analysis of the landing process than a low-precision model. A higher-precision simulation model deserves a larger correlation, as does the ground test. Therefore, experts should conduct the assessment rigorously to obtain a rational estimate. If the corresponding simulation model or ground test method is modified, the correlation should also be changed.

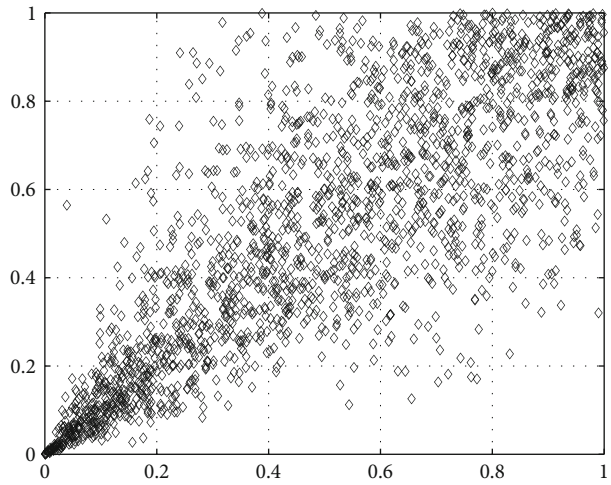

Figure 9: Lower-tail behavior of Clayton copula.

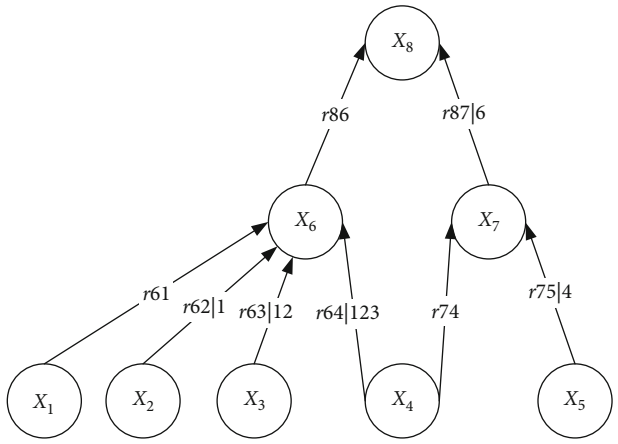

Figure 10: Vine-BN of the landing reliability network.

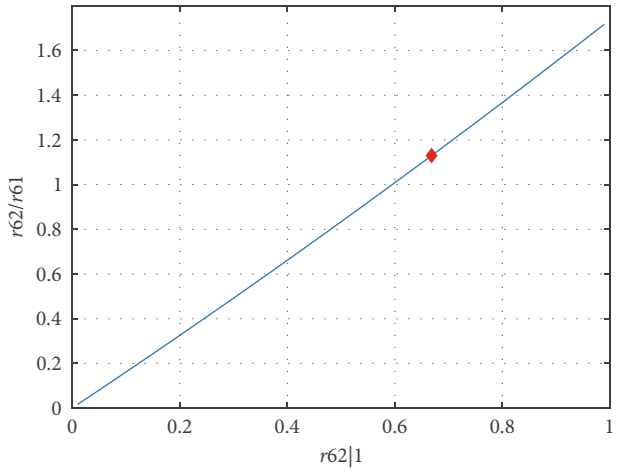

Figure 11: $r62/r61$ versus $r62 \mid 1$, given $P_1 = 0.670$.

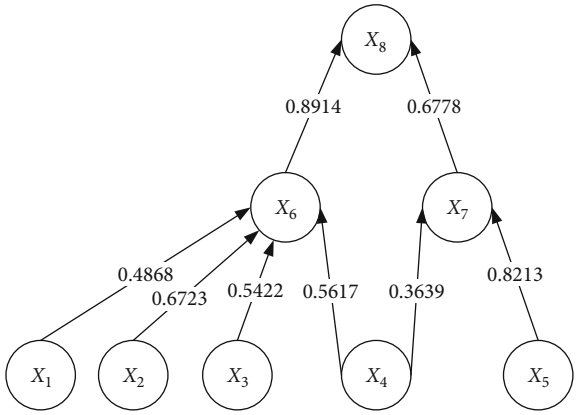

Figure 12: Quantified network.

5. Network Model Implementation for Landing Reliability

After quantification, the network can be updated in the forward and backward directions. Forward propagation inferred the distribution of the leaf nodes from the root nodes; i.e., the landing reliability is estimated in light of ground test and simulation. Backward propagation updates the other nodes' distribution under the given leaf nodes, and it is aimed at exploring the most probable causes in fault diagnosis while, in our studies, it works to identify the key performance metrics related to landing reliability. In the subsequent section, we will illustrate the network application from the two propagations in the landing reliability assessment.

5.1. Forward Propagation Analysis: Reliability Prediction and Test Times Decision. Once the simulations and ground test data are available, the network can be updated accordingly. Figure 13 depicts the general updating process. The estimation of the performance metrics described in Section 4 is taken as evidence to update the network. The leaf node distribution is also the fusion of simulation and ground test. The beta distribution will be adopted to fit the fusion result so that decision-making of field test times can be implemented.

The distribution of the leaf node will be utilized as the prior distribution to yield the posterior distribution with field data. Let R denote the landing reliability, and let $\pi(R)$ denote the probability density of the distribution of the leaf node, which can be expressed by the beta distribution:

$$\pi(R) = \beta(R|a,b) = \frac{1}{B(a,b)} R^{a-1}(1-R)^{b-1}, \quad 0 < R < 1. \tag{17}$$

After updating, parameters a and b can be determined by the leaf node's sample through the following equation:

$$a = \frac{\mu_R^2(1-\mu_R) - \sigma_R^2\mu_R}{\sigma_R^2}, \; b = \frac{\mu_R(1-\mu_R)^2 - \sigma_R^2(1-\mu_R)}{\sigma_R^2}, \tag{18}$$

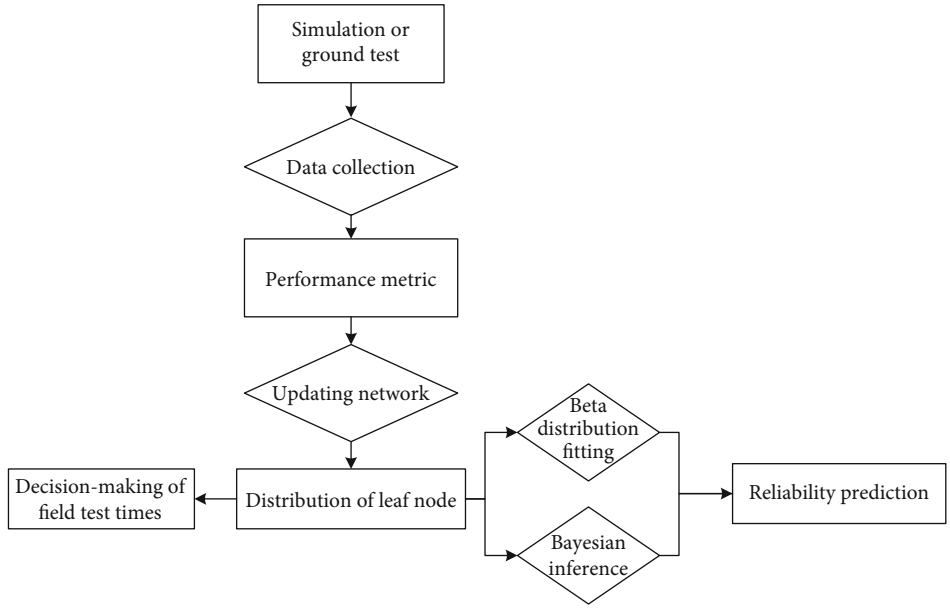

Figure 13: Forward propagation process.

where μ_R is the sample mean and σ_R is the variance. When field test data are available, the posterior distribution of landing reliability can be obtained directly by taking $\pi(R)$ as the prior distribution. Assume that n airdrop tests have been carried out. s is the number of successful tests, and the posterior distribution of R is [43]

$$\pi(R|n,s) = \beta(R|a+s, n-s+b). \tag{19}$$

The decision-making of field test times can be conducted from the posterior distribution. Given the lower bound of the landing reliability R_L and confidence level γ, the zero-failure test times N can be determined by the following equation:

$$\int_{R_L}^{1} \beta(R|a+N, b)dR = \gamma. \tag{20}$$

In the forward propagation section, the following analysis will be presented from two aspects: reliability prediction and test times decision. The use of forward propagation for reliability prediction and test times decision has two advantages. First, expert opinions are reasonable measurements of simulation models or test methods, which can avoid the unreasonable results provided only by MCS. Second, the fusion of multisource information, which has complementarity due to the diverse sources, can perform reliability prediction and test times decision-making more reasonably. In the following, we will illustrate the two advantages from single-source and multisource forward propagation, respectively. Note that the single-source information in the following section refers to the root node of the network, that is, the amount of simulation or test information adopted. However, since the network is quantified by expert opinions, the expert opinion information is integrated even under single-source information.

Table 3: Simulation result under different T_s.

T_s	Simulation result (success cases, failure cases)	Point estimation	Interval estimation, confidence level of 0.9
2 kN	(437, 563)	0.437	[0.4169, 1]
4 kN	(734, 266)	0.734	[0.7160, 1]
6 kN	(865, 135)	0.865	[0.8510, 1]
8 kN	(948, 52)	0.948	[0.9388, 1]

5.1.1. Reliability Prediction and Test Time Decision Based on Single-Source Information. X_1 represents the release probability calculated by Wang et al.'s model [31], which took the motion state of the parachutes and the wind field as random factors to perform MCS to investigate the landing. For details, we refer the reader to the appendix. The system's performance can be improved by adjusting key design parameters in the design stage. Wang et al. pointed out that the design release force T_s has considerable influence on the release process. Table 3 shows simulation results under different T_s (1000 times MCS). The point and interval estimations of X_1 are also given.

If the landing reliability is evaluated only by taking the release simulation results, according to Table 3, the lower bound of the landing reliability can reach 0.9388 by simply adjusting the design release force to 8 kN, which is far from the actual engineering experience. For a more reasonable evaluation of landing reliability, the simulation results are substituted into node X_1 in the network for forward propagation. Theoretically, the network can be updated with values, intervals, or distributions on $[0, 1]$. Here, we took the point estimation as an example to illustrate.

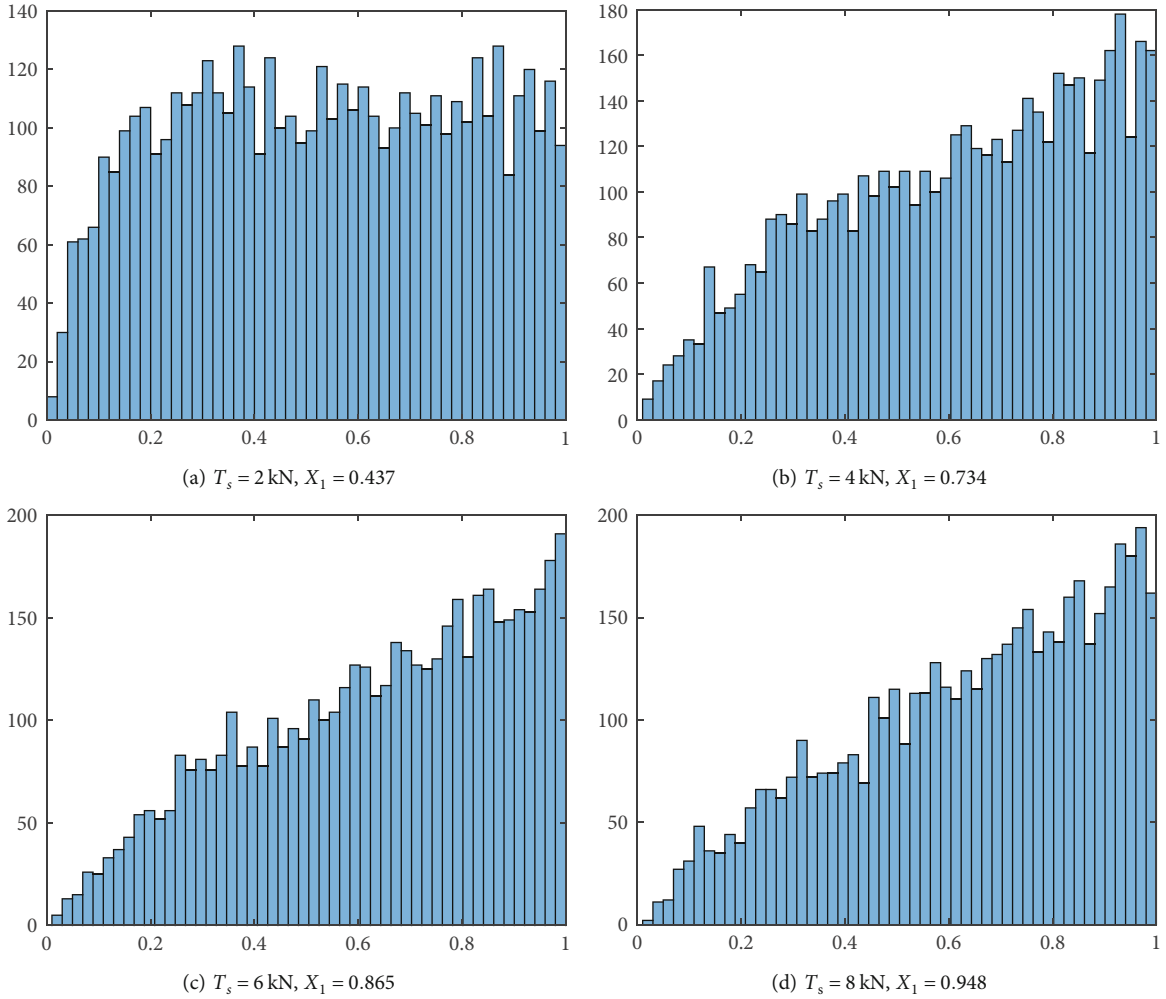

Figure 14: Distribution of leaf node by updating with simulation results.

Table 4: Reliability prediction and test times decision based only on release simulation, confidence level of 0.9 and lower-bound reliability of 0.8.

T_s	Point estimation	Interval estimation, confidence level of 0.9	Zero-failure test times	Zero-failure test times, binomial data (airdrop test data) only
2 kN	0.5292	[0.1576, 1]	9.889	10.32
4 kN	0.6183	[0.2482, 1]	8.831	
6 kN	0.6322	[0.2645, 1]	8.573	
8 kN	0.6451	[0.2830, 1]	8.450	

Figure 14 presents the distribution of the leaf node under four different design release forces. The figure shows that the sample of leaf nodes is slightly concentrated in the right region as the release design force increases. Table 4 shows the results of reliability prediction and field test times decision based on the distribution of leaf nodes for a given lower bound on reliability of 0.8 and confidence level of 0.9. Also, the test times required for reliability assessment based solely on binomial data (airdrop test) is presented. The results indicate that landing reliability can be improved by increasing the design release force, but the improvement is quite limited. The point estimate improves only from 0.5292 to 0.6451, while the lower bound improves from 0.1576 to 0.2830 as the design release force increases from 2 kN to 8 kN. The zero-failure test times are reduced from 9.889 to 8.450, which is quite limited since only 10.32 zero-failure tests are required based solely on the airdrop test.

The results manifest that the information for landing performance provided by the release simulation is quite limited, and it is difficult to make a definitive judgment on the

landing performance based on the simulation results. This is due to the roughness of the release simulation model. When quantifying the network according to the expert opinions, wherein the experts estimatedP_1 of Equation (15) based on question 1, only a conservative value of 0.670 was given. A crude simulation model can provide relatively limited information, whereas the results of a high-precision simulation model should be given sufficient attention. According to the expert opinion, a more accurate simulation model would correspond to a larger P_1, thus affecting the reliability prediction and test times decision. To illustrate it from a quantitative point of view, we show reliability prediction and test times decision under different expert opinions. The release simulation probability is assumed to be 0.95; that is, $X_1 = 0.95$ is used to update the network.

From Figure 15, we can see that the lower-bound reliability increases as the experts estimate a larger P_1, while the zero-failure test times decrease as the P_1 increases. Specifically, when the experts assess P_1 to be 0.55, the lower-bound reliability is only 0.142 and the zero-failure test times are 8.724, which is almost the same as the results without any prior information since the simulation model is too crude to provide valid information. Conversely, the lower-bound reliability increases to 0.6187 and the test times drop to 6.018 when experts estimate P_1 to be 0.95, in which case the experts consider the simulation model with high accuracy. The analysis demonstrates that expert opinion, which measures the effectiveness of a simulation or ground test, has a significant impact on the reliability prediction and test times decision. Therefore, experts should carefully and comprehensively analyze the rationality of simulation models and test methods.

It is important to note that even with the expert evaluation of $P_1 = 0.95$, the lower bound of the landing reliability is only 0.6178, which still requires 6.018 zero-failure drop tests, while relying solely on drop tests requires only 10.32 tests. This is due to two reasons. First, the performance metric for node 1 only concerns rollover accidents caused by the release process, and it does not investigate accidents due to overload; that is, node 1 is connected only to faulty node 6. Second, the accuracy of the simulation model is limited. As a result, it is necessary to integrate multisource information to assess landing reliability from multiple perspectives.

5.1.2. Reliability Prediction and Test Time Decision Based on Multisource Information Fusion. The prediction of landing reliability will be more reasonable and accurate if more information is available. To demonstrate the feasibility of vine-BN in information fusion, Table 5 shows three information cases, and Figure 16 shows the corresponding distribution of the leaf node under these cases.

Figure 16(a) shows the leaf node distribution corresponding to case 1. Due to the satisfactory performance of all metrics, the samples are concentrated in the right area of the picture, and the lower bound of landing reliability is 0.8327. Figure 16(b) shows an opposite result to Figure 16(a), where all the performance metrics have a poor state: the samples concentrate in the left area of the picture, and the lower bound of landing reliability is only 0.0638. Note that the samples in

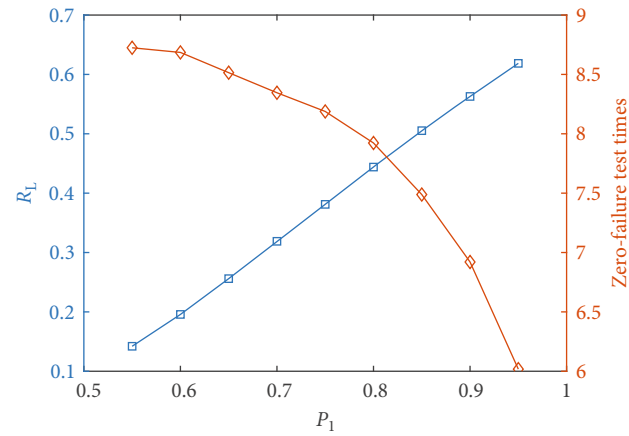

Figure 15: Reliability prediction and test times decision with different expert opinions, confidence level of 0.9, and lower-bound reliability of 0.8.

Table 5: Reliability prediction cases using evidence from simulation and ground test.

Evidence	Case		
	No. 1	No. 2	No. 3
RNS	0.9	0.2	0.9
LERTGT	0.9	0.2	0.9
RNDT	0.9	0.2	0.9
DTRH	0.9	0.2	0.2
DTO	0.9	0.2	0.2

Figure 16(b) are more concentrated than those in Figure 16(a). This is due to the lower-tail characteristic of the Clayton function; i.e., it is more reasonable to identify the low reliability of the system when the simulation or ground test shows poor performance. Figure 16(c) shows the distribution under case 3. Although the three metrics show good performance, the lower bound is only 0.5620 due to the poor performance of two metrics.

From Table 6, we can see that out of the three cases, only case 1 requires the minimum number of zero-failure field tests. For case 2, since both simulation and test results indicate poor landing performance, more field tests are needed to prove that the reliability of the system is up to standard, but this is only the result of theoretical calculations. In practical engineering, it is also impossible to have more than 100 zero-failure airdrop tests if the simulation or ground test performance metrics fail to meet the performance target.

The essence of integrating multiple information is to investigate the landing reliability of the system from different perspectives. Combining with the results of case 1 in Table 6 and Table 4, it can be seen that when field tests are insufficient, more information can be fused to reduce the zero-failure test times. To illustrate this quantitatively, we present Figure 17.

Figure 17 shows the landing reliability as a function of the number of zero-failure test times under different

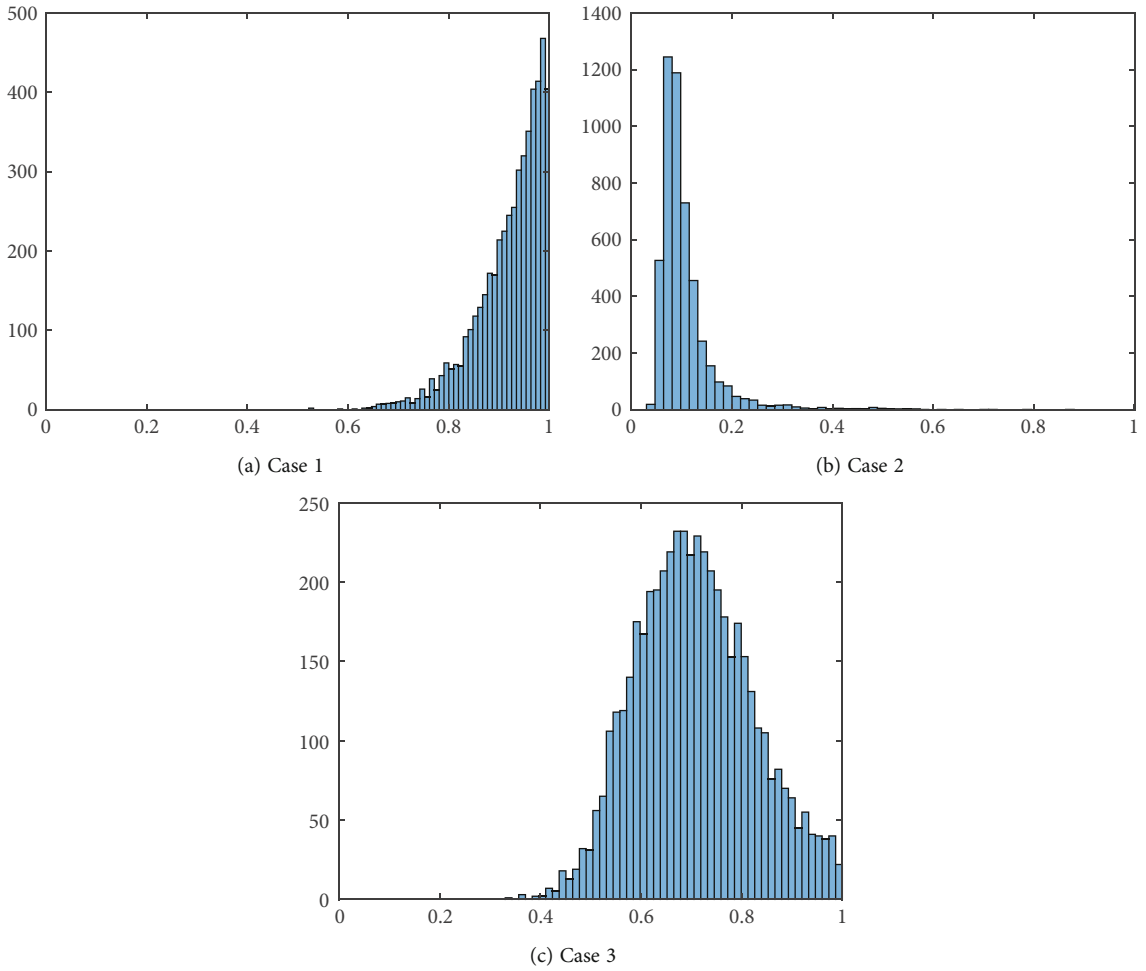

Figure 16: Distribution of leaf node by updating with multisource information.

Table 6: Reliability prediction and test times decision based on fusion of multisource information, confidence level of 0.9, and lower-bound reliability of 0.8.

Case	Point estimation	Interval estimation, confidence level of 0.9	Zero-failure test times	Zero-failure test times, binomial data (airdrop test data) only
Case 1	0.9234	0.8327	0	
Case 2	0.1061	0.0638	110.6	10.30
Case 3	0.7078	0.5620	19.60	

information fusions. It can be seen that the number of zero-failure tests decreases as the information fusion increases. Specifically, when fusing five pieces of information and achieving 1 for each performance metric, 8.324 more zero-failure field tests are required to give a lower bound of 0.9 for landing reliability, while 19.33 zero-failure field tests are still needed when evaluated from simulations alone. It should be noted that the gap between different information fusions gradually narrows as the number of field tests increases. In addition, if the number of field tests is large, R_L tends to be stable. This is because, when the number of

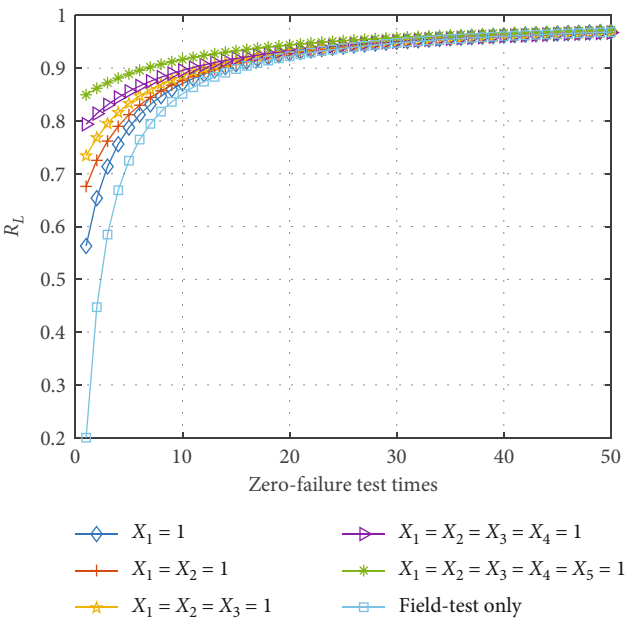

Figure 17: Lower bound of landing reliability versus zero-failure test times with different information fusions and confidence level of 0.9.

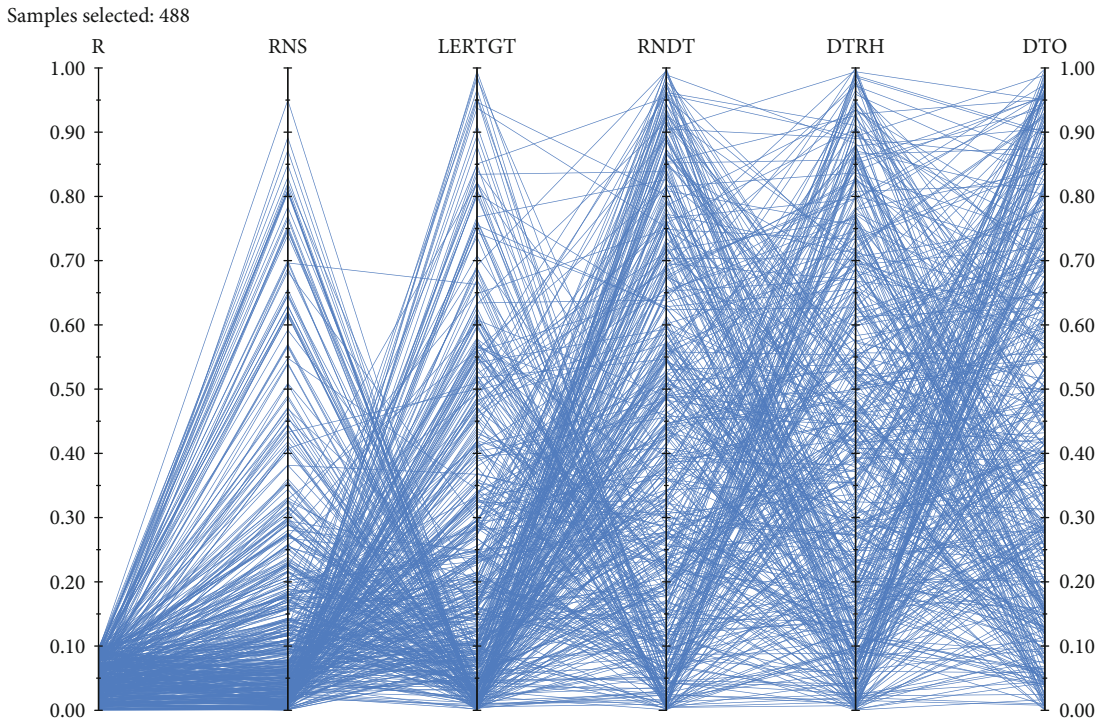

Figure 18: Conditional cobweb plot and landing reliability condition on [0, 0.1].

field tests is small, the assessment mainly depends on the simulation and ground test, so the R_L between the two methods will be significantly different. With the increase of field tests, the knowledge of landing mainly depends on field tests, so the gap gradually narrows. Since the field samples are usually limited, more information can be fused by the network, resulting in a significant reduction in the cost and workload of testing.

Note that different performance metrics have different contributions to landing reliability, which will be discussed in the next section.

5.2. Backward Propagation Analysis: Identification of Key Performance Metrics. As mentioned above, backward propagation updates the network under the given landing reliability. The variations of the root nodes indicate the degree that contributes to landing reliability. To be specific, we investigate the variation of performance metrics' distribution according to the extremely low landing reliability. The performance metrics' distribution changes significantly, indicating that when the reliability of performance measures is low, landing accidents are likely to occur. Therefore, more effort should be made to improve the performance metric in the design stage. In the following, we will illustrate the backward propagation from both qualitative and quantitative points of view.

5.2.1. Qualitative Analysis. Identifying the most critical variables within a given range of target variables is essentially a local probabilistic sensitivity analysis [44]. Cooke and van Noortwijk [45] introduced a visual tool for sensitivity analysis, called the cobweb plot. The cobweb plot can intuitively show the relationship between multivariate variables based on a large number of multivariate samples, and it has been applied to the reliability analysis of underwater tunnels [29], complex electronic systems [46], subsea pipelines [47], etc. Unigraph provides cobweb plot functions and is a postprocessing module of Uninet, but is also available as a standalone software. Uninet is a calculation software developed by Ababei and Lewandowski [48] based on vine copula and vine-BN theory, and it is theoretically supported by Delft University of Technology. An academic version of the software is available at https://lighttwist-software.com/uninet/. In the following, we will illustrate the qualitative analysis via Unigraph. First, we sample from the landing reliability network and import the samples into Unigraph, then condition the landing reliability on interval $[0, 0.1]$.

As Figure 18 shows, on top of each vertical axis label are the names of the performance metrics. The leftmost axis represents landing reliability. The remaining four labels, from left to right, correspond to the root nodes' names of the network shown in Figure 8(b). Each axis marks the percentile sample of each variable. Since all nodes in the network are defined as uniformly distributed on $[0, 1]$, the samples generated by sampling from the network are the percentile samples. The blue lines connect each pair of sample on the vertical axes. It is intuitive to see that the samples of RNS and LERTGT are concentrated at the bottom of the axis, while the other samples are distributed nearly uniformly along the axis. A preliminary conclusion can be drawn that RNT and LERTGT have a significant influence on landing reliability according to Figure 18. Therefore, to improve landing reliability, the parachute-separation probability calculated from the release simulation model should first be

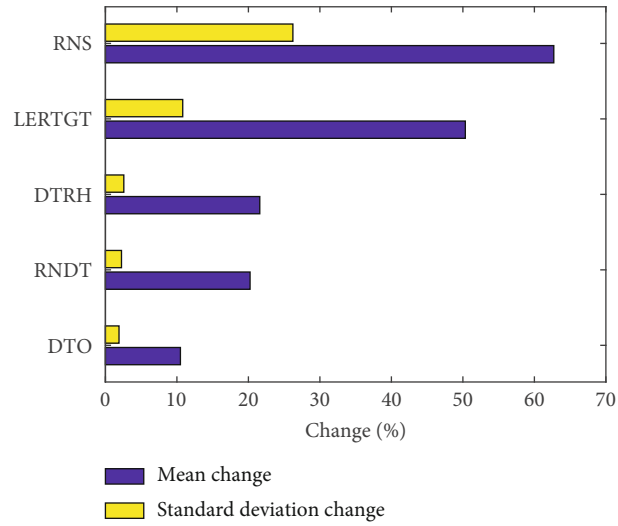

Figure 19: Change of statistical characteristics during backward propagation.

increased, together with a reduction in the response time of the latch ejection.

In this paper, we present a simplified network based on specific ground test and simulation information. If more information is available and multiple failure modes are considered simultaneously, as shown in Figure 8(a) for complex network structures, the identification function of the cobweb graph would be prominent.

5.2.2. Quantitative Analysis. Figure 19 shows the variation of mean and standard deviation with the landing reliability condition on $[0, 0.1]$. Note that the variation is calculated by $|(\text{updated} - \text{prior})/\text{prior}|$, where the prior distribution is uniform.

As shown, the sequence of contribution to landing reliability is RNS, LERTGT, DTRH, RNDT, and DTO. RNS and LERTGT experience significant changes (62.72% and 26.22% and 50.34% and 10.81%, respectively). Therefore, more attention should be paid to the performance metrics of RNS and LERTGT in the design stage. Specifically, the corresponding design parameters, such as the spring stiffness of the release unit and the design release force, should be adjusted first to meet the performance requirements. However, the performance metrics are also influenced by different design parameters, which are connected in complex ways. Therefore, the network can be further extended to set the design parameters as root nodes, while the metrics as intermediate nodes, to identify the key design parameters.

For illustration, Figure 20 shows an extension of the general network structure, where from the bottom to the top are the design parameter layer, the performance metric layer, and the failure mode layer. The present work is limited to exploring the correlation between performance metrics and failure modes. In practical engineering applications, the design parameter layer should be considered in order to determine the key parameters more directly. The definition of nodes for design parameters and the elicitation of correlations between performance metrics and design parameters will be challenging and require further research.

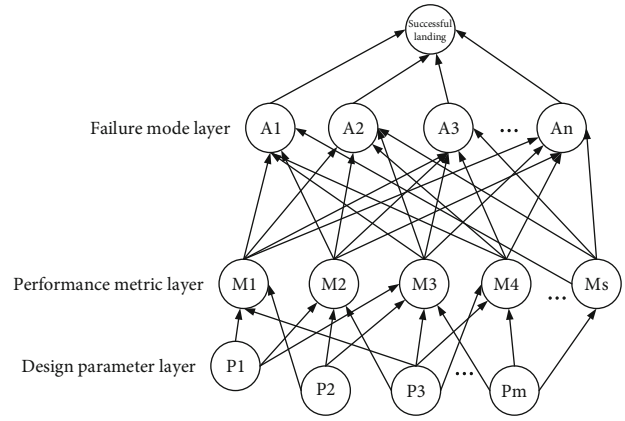

Figure 20: Extensions to the general network structure.

6. Conclusion and Future Work

(1) A methodology for assessing the landing reliability of airdrop systems by fusing multiple-source information based on vine-BN is proposed. For illustration, a network is developed based on specified ground tests and simulation for an HCADS. The network structure is determined by the correlation between the performance metrics of simulation or ground tests and landing-failure modes. Nodes in the network are defined as random variables on $[0, 1]$, and the correlation coefficients on arcs are elicited by expert opinions

(2) The forward propagation under different information cases shows that vine-BN is a reasonable tool for fusing multisource information. Through the fusion results, landing reliability can be predicted in the design stage. Decision-making regarding the field test times can be performed, and the field test times are reduced remarkably. The methodology can significantly reduce the cost and workload of the test

(3) The backward propagation only recognizes the key performance metrics; it is not intuitive in system design. In order to provide a more intuitive analysis, the key design parameters should be identified, and the network should be extended. How to define the design parameter nodes and how to derive the correlations at the arcs of the design parameters are the most critical issues and require further research

Appendix

Figure 21 is the schematic diagram for the release simulation model. The parachute-connecting rope and the cargo hanger rope are simplified to a single unit, and the release unit is a point on it. The influence of the cushion process will not be considered in this model.

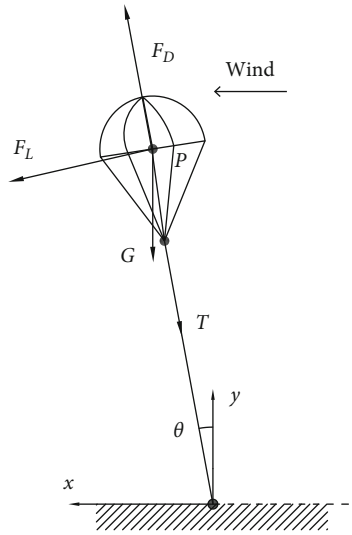

Figure 21: Force analysis of the simplified system.

The kinetic equation is

$$\left(m_p + m_f\right)\begin{bmatrix}\ddot{x}_p\\ \ddot{y}_p\end{bmatrix} = \mathbf{F}_L + \mathbf{F}_D + \mathbf{T} + \mathbf{G}_p, \tag{A.1}$$

where m_p and m_f is the parachute mass and added mass, respectively; the expression for m_f is

$$m_f = k_f \rho (\mathrm{CA})^{3/2}. \tag{A.2}$$

k_f is the added mass coefficient, and its value can be 0.66 [49]. The tension force T is as follows:

$$T = \begin{cases} k(L - L_0), & (L > L_0), \\ 0, & (L \le L_0). \end{cases} \tag{A.3}$$

L_0 is the original length of the parachute-connecting rope and L is the instantaneous length during landing, which can be calculated by Equation (A.3).

$$L \doteq \sqrt{x_p^2 + y_p^2}. \tag{A.4}$$

The stiffness k can be calculated by

$$k = \frac{T_0}{\Delta L_0}. \tag{A.5}$$

T_0 is the tension in the parachute-connecting rope when the system is in a stable descending state, and it equals the gravity of the cargo. ΔL_0 is the elongation before landing, and it is a given parameter.

Table 7: List of the calculation parameters.

m_c (kg)	T_s (kN)	L_0 (m)	ΔL_0 (m)	A_0 (m^2)
8200	5	65	6.5	2584

F_L and F_D are the lift force and drag force, respectively, expressed as

$$F_L = \frac{1}{2}\rho v^2 C_L A_0,\ F_D = \frac{1}{2}\rho v^2 C_D A_0 \tag{A.6}$$

where C_L and C_D are the lift and drag coefficients, respectively, and for the relationship with the attack angle, we can refer to reference [50].

In this model, we only consider the case where the wind field is horizontal and the airspeed of the parachute can be calculated by

$$v = \sqrt{\left(\dot{x}_p + u_0\right)^2 + \dot{y}_p^2}, \tag{A.7}$$

where u_0 is the wind speed. T can be calculated through the above equation. If T satisfies Equation (A.7), the release process is successful.

$$T < T_s. \tag{A.8}$$

T_s is the design release force in system design. If T is greater than T_0 during landing, it indicates that the cargo may be pulled up, in which case, the rollover may occur; thus, the release process can be regarded as a failure.

The initial swing angle θ_0, swing speed v_{p0}, and falling speed $\dot{y}_0$ of the system with the influence of the wind contribute to the uncertainty of landing jointly. The release probability, i.e., the probability of no rollover, can be calculated using MCS.

According to engineering experience, it is assumed that the variables follow the following distribution:

$$\theta_0 \sim N\left(0, 3.33^2\right)\dot{y}_0 \sim N\left(-7, 0.33^2\right)u_0 \sim N\left(7, 2^2\right). \tag{A.9}$$

The approximately linear relationship between v_{p0} and θ_0 is taken:

$$v_{\mathrm{p0}} = \pm v_{\mathrm{p0\ max}}\left(1 - \left|\frac{\theta_0}{10}\right|\right). \tag{A.10}$$

Other parameters are shown in Table 7.

Data Availability

The data used to support the findings of the manuscript (titled "Landing Reliability Assessment of Airdrop System based on Vine-Bayesian Network") have been deposited in the "figshare" repository (10.6084/m9.figshare.20304609.v1).

Conflicts of Interest

The authors declare that they have no conflicts of interest.

References

[1] K. Bergeron, M. Ghoreyshi, and A. Jirasek, "Simulation of C-130 H/J troop doors and cargo ramp flow fields," *Aerospace Science and Technology*, vol. 72, pp. 525–541, 2018.

[2] M. Ghoreyshi, K. Bergeron, T. M. Rose, A. Jirasek, and G. Noetscher, "Personnel airdrop extraction simulations for C-130 H/J," in *AIAA Scitech 2020 Forum*, Orlando, FL, 2020.

[3] M. Ghoreyshi, T. M. Rose, N. J. Thompson, A. Jirasek, G. Noetscher, and K. Bergeron, "A paratrooper model sensitivity analysis for personnel airdrop," in *AIAA Scitech 2021 Forum*, Virtual Event, 2021.

[4] H. T. Wang, "Dynamic modeling and simulation of whipping phenomenon for large parachute," *AIAA Journal*, vol. 56, no. 10, pp. 4049–4059, 2018.

[5] K. Takizawa, S. Wright, C. Moorman, and T. E. Tezduyar, "Fluid–structure interaction modeling of parachute clusters," *International Journal for Numerical Methods in Fluids*, vol. 65, no. 1-3, pp. 286–307, 2011.

[6] A. M. Cinnamon, E. A. Miller, and J. Mudrak, "Analysis of performance metrics for precision airdrop," in *24th AIAA Aerodynamic Decelerator Systems Technology Conference*, Denver, Colorado, 2017.

[7] J. Wachlin and M. Costello, "Simulation of the landing dynamics of a guided airdrop system," in *AIAA Aviation 2019 Forum*, Dallas, Texas, 2019.

[8] Y. Dong, J. Ding, C. Wang, H. Wang, and X. Liu, "Soft landing stability analysis of a Mars lander under uncertain terrain," *Chinese Journal of Aeronautics*, vol. 35, no. 11, pp. 377–388, 2022.

[9] L. Witte, R. Roll, J. Biele, S. Ulamec, and E. Jurado, "Rosetta lander Philae - landing performance and touchdown safety assessment," *Acta Astronautica*, vol. 125, pp. 149–160, 2016.

[10] T. J. Lee, J. McKinney, and M. Farkas, "Airbag landing impact test/analysis for the crew exploration vehicle," in *49th AIAA/ASME/ASCE/AHS/ASC Structures, Structural Dynamics, and Materials Conference, 16th AIAA/ASME/AHS Adaptive Structures Conference,10th AIAA Non-Deterministic Approaches Conference, 9th AIAA Gossamer Spacecraft Forum, 4th AIAA Multidisciplinary Design Optimization Specialists Conference*, Schaumburg, IL, 2008.

[11] H. Wang, H. Hong, J. Y. Li, and Q. Rui, "Study on multi-objective optimization of airbag landing attenuation system for heavy airdrop," *Defence Technology*, vol. 9, no. 4, pp. 237–241, 2013.

[12] X. Liu, Z. Zhang, and Z. Zhao, "The uncertain optimisation of buffering characteristics of landing airbag in manned airdrop," *International Journal of Crashworthiness*, vol. 18, no. 3, pp. 225–236, 2013.

[13] X. H. Fu, "Analysis on characteristics of structural impact response of airborne armored vehicle in landing process," *IOP Conference Series: Materials Science and Engineering*, vol. 484, 2019.

[14] B. C. Fuqua, "ENRE 655 class project. Development of the initial main parachute failure probability for the constellation program (CxP)," in *Orion Crew Exploration Vehicle (CEV) Parachute Assembly System (CPAS)*, Houston, TX, 2010.

[15] X. Gao, Q.-B. Zhang, and Q.-G. Tang, "Reliability assessment of slot-parachute inflation based on Bayes theory," *Journal of Statistical Computation and Simulation*, vol. 84, no. 6, pp. 1159–1172, 2014.

[16] F. Ma, H. Lei, W. Wang, J. Liu, and L. Jin, "Research on reliability assessment method of emergency escape parachute," *Journal de Physique*, vol. 1544, no. 1, article 012185, 2020.

[17] R. A. Machin, T. E. Fisher, C. T. Evans, and C. E. Stewart, "Human rating the Orion parachute system," in *21st AIAA Aerodynamic Decelerator Systems Technology Conference and Seminar*, Dublin, Ireland, 2011.

[18] J. Sun, H. Zuo, K. Liang, and Z. Chen, "Bayesian network-based multiple sources information fusion mechanism for gas path analysis," *Journal of Propulsion and Power*, vol. 32, no. 3, pp. 611–619, 2016.

[19] J. Chen and Y. Liu, "Multimodality data fusion for probabilistic strength estimation of aging materials using Bayesian networks," in *AIAA Scitech 2020 Forum*, Orlando, FL, 2020.

[20] M. Junghans and H.-J. Jentschel, "Qualification of traffic data by Bayesian network data fusion," in *2007 10th International Conference on Information Fusion*, Quebec, QC, Canada, 2007.

[21] B. Cai, Y. H. Liu, Q. Fan et al., "Multi-source information fusion based fault diagnosis of ground-source heat pump using Bayesian network," *Applied Energy*, vol. 114, pp. 1–9, 2014.

[22] D. Kurowicka and R. M. Cooke, "Distribution-free continuous Bayesian belief nets," in *Modern statistical and mathematical methods in reliability*, vol. 10, pp. 309–322, World Scientific Publishing, 2005.

[23] T. Bedford and R. M. Cooke, "Vines - a new graphical model for dependent random variables," *The Annals of Statistics*, vol. 30, no. 4, pp. 1031–1068, 2002.

[24] T. Bedford and R. M. Cooke, "Probability density decomposition for conditionally dependent random variables modeled by vines," *Annals of Mathematics and Artificial Intelligence*, vol. 32, pp. 245–268, 2001.

[25] O. Morales-Napoles, D. J. Delgado-Hernández, D. DeLeón-Escobedo, and J. C. Arteaga-Arcos, "A continuous Bayesian network for earth dams' risk assessment: methodology and quantification," *Structure and Infrastructure Engineering*, vol. 10, no. 5, pp. 589–603, 2014.

[26] A. A. Zilko, D. Kurowicka, and R. M. P. Goverde, "Modeling railway disruption lengths with copula Bayesian networks," *Transportation Research Part C: Emerging Technologies*, vol. 68, pp. 350–368, 2016.

[27] D. J. Lee and R. Pan, "A nonparametric Bayesian network approach to assessing system reliability at early design stages," *Reliability Engineering and System Safety*, vol. 171, pp. 57–66, 2018.

[28] M. A. Mendoza-Lugo, D. J. Delgado-Hernández, and O. Morales-Napoles, "Reliability analysis of reinforced concrete vehicle bridges columns using non-parametric Bayesian networks," *Engineering Structures*, vol. 188, pp. 178–187, 2019.

[29] Y. Pan, S. Ou, L. Zhang, W. Zhang, X. Wu, and H. Li, "Modeling risks in dependent systems: a copula-Bayesian approach," *Reliability Engineering and System Safety*, vol. 188, pp. 416–431, 2019.

[30] J. Sun, F. Wang, Z. Li, D. Ren, and M. Yu, "A new hybrid copula-based nonparametric Bayesian model for risk assessments of water inrush," *Quality and Reliability Engineering International*, vol. 38, no. 4, pp. 1957–1976, 2022.

[31] Y. W. Wang, C. X. Yang, P. Ke, and X. S. Yang, "Probability analysis on parachute ground release for cargo airdrop system," *Acta Aeronautica et Astronautica Sinica*, vol. 31, no. 2, pp. 265–270, 2010.

[32] J. McCann, T. C. DePauw, J. McKinney, P. Ferguson, M. Weber, and T. P. Taylor, "Boeing CST-100 landing and

recovery system design and development an integrated approach to landing," in *AIAA SPACE 2013 Conference and Exposition*, San Diego, CA, 2013.

[33] L. S. Shook, R. B. Timmers, and J. Hinkle, "Second generation airbag landing system for the Orion crew module," in *20th AIAA Aerodynamic Decelerator Systems Technology Conference and Seminar*, Seattle, Washington, 2009.

[34] R. B. Nelsen, *An Introduction to Copulas*, Springer, New York, N.Y, 2nd edition, 2007.

[35] H. Joe, "Families of m-variate distributions with given margins and $m(m-1)/2$ bivariate dependence parameters," in *Distributions with Fixed Marginals and Related Topics*, vol. 128 of Lecture Notes-Monograph Series, pp. 120–141, 1996.

[36] K. Aas, C. Czado, A. Frigessi, and H. Bakken, "Pair-copula constructions of multiple dependence," *Insurance: Mathematics & Economics*, vol. 44, no. 2, pp. 182–198, 2009.

[37] D. Kurowicka and R. M. Cooke, *Uncertainty Analysis with High Dimensional Dependence Modelling*, John Wiley & Sons Ltd, Chichester, 2006.

[38] D. Kurowicka and R. M. Cooke, "Sampling algorithms for generating joint uniform distributions using the vine-copula method," *Computational Statistics and Data Analysis*, vol. 51, no. 6, pp. 2889–2906, 2007.

[39] A. M. Hanea, "Algorithms for non-parametric Bayesian belief nets, [Ph.D. thesis]," in *Applied Mathematics*, Delft University of Technology, Delft, 2008.

[40] O. Morales-Napoles, D. Kurowicka, and A. Roelen, "Eliciting conditional and unconditional rank correlations from conditional probabilities," *Reliability Engineering and System Safety*, vol. 93, no. 5, pp. 699–710, 2008.

[41] J. V. Deshpande, U. Naik-Nimbalkar, and I. Dewan, *Nonparametric Statistics*, World Scientific, Singapore, 2018.

[42] J. H. Sigurdsson, L. A. Walls, and J. L. Quigley, "Bayesian belief nets for managing expert judgement and modelling reliability," *Quality and Reliability Engineering International*, vol. 17, no. 3, pp. 181–190, 2001.

[43] M. S. Hamada, A. G. Wilson, S. Reese, and H. F. Martz, *Bayesian reliability*, vol. 15, Springer, New York, 2008.

[44] R. M. Cooke and J. M. van Noortwijk, "Local probabilistic sensitivity measures for comparing FORM and Monte Carlo calculations illustrated with dike ring reliability calculations," *Computer Physics Communications*, vol. 117, no. 1-2, pp. 86–98, 1999.

[45] R. Cooke and J. van Noortwijk, "Graphical Methods for Uncertainty and Sensitivity Analysis," in *Sensitivity Analysis*, A. Saltelli, K. Chan, and E. M. Scott, Eds., pp. 245–266, Wiley, 2000.

[46] B. Sun, Y. Li, Z. Wang, D. Yang, Y. Ren, and Q. Feng, "A combined physics of failure and Bayesian network reliability analysis method for complex electronic systems," *Process Safety and Environmental Protection*, vol. 148, pp. 698–710, 2021.

[47] X. Li, Y. Liu, R. Abbassi, F. Khan, and R. Zhang, "A copula-Bayesian approach for risk assessment of decommissioning operation of aging subsea pipelines," *Process Safety and Environmental Protection*, vol. 167, pp. 412–422, 2022.

[48] D. A. Ababei and D. Lewandowski, "UniNet help," https://lighttwist-software.com/uninet.

[49] L. R. Wang, *Theory and Application of Parachute*, Aerospace Press, Beijing, 1997.

[50] V. N. Dobrokhodov, O. A. Yakimenko, and C. J. Junge, "Six-degree-of-freedom model of a controlled circular parachute," *Journal of Aircraft*, vol. 40, no. 3, pp. 482–493, 2003.